The Influence of the Aggregation of a Carbazole Thiophene Cyanoacrylate Sensitizer on Sensitized Photocurrents on ZnO Single Crystals.

ARTICLE *in* LANGMUIR · JULY 2013

Impact Factor: 4.46 · DOI: 10.1021/la400493v · Source: PubMed

2 AUTHORS:

Alexander B Nepomnyashchii
Northwestern University
22 PUBLICATIONS **334** CITATIONS
SEE PROFILE

Bruce A Parkinson
University of Wyoming
251 PUBLICATIONS **7,008** CITATIONS
SEE PROFILE

THE JOURNAL OF PHYSICAL CHEMISTRY Letters

Letter

pubs.acs.org/JPCL

Photosensitization of Single-Crystal ZnO by a Conjugated Polyelectrolyte Designed to Avoid Aggregation

Xuzhi Zhu,[†] Alexander B. Nepomnyashchii,[§] Adrian E. Roitberg,[†] B. A. Parkinson,*[,§] and Kirk S. Schanze*[,†]

[†]Department of Chemistry, Center for Macromolecular Science and Engineering, University of Florida, P.O. Box 117200, Gainesville, Florida, 32611-7200, United States

[§]Department of Chemistry, School of Energy Resources, University of Wyoming, Laramie, Wyoming, 82071, United States

Supporting Information

ABSTRACT: A conjugated polyelectrolyte (CPE) based on a poly(phenylene ethynylene) backbone designed to avoid interchain aggregation was adsorbed onto n-type zinc oxide (0001) single crystals. Photophysical, atomic force microscopy, and photoelectrochemical measurements confirm the absence of aggregation in solution and on ZnO single-crystal surfaces. At high surface coverage on the ZnO surface, individual polymer chains are resolved, and photocurrent efficiency measurements suggest that charge injection occurs with modest efficiency.

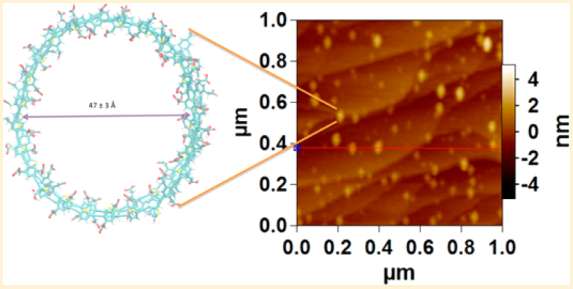

SECTION: Surfaces, Interfaces, Porous Materials, and Catalysis

Conjugated polyelectrolytes (CPEs) are of interest as sensitizers in dye-sensitized solar cells (DSSCs), owing to their large absorption cross section, tunable band gap, and charge and exciton transport properties.[1−4] The interaction of CPE chains with a metal oxide semiconductor surface can also be controlled through the degree of functionalization with polar and ionic functionality on the polymer backbone. The morphology of CPE chains and aggregates at the polymer−semiconductor interface, where charge separation occurs, plays a pivotal role in the charge injection efficiency and spectral response of the photocurrent.[5,6] For example, previous studies suggest that exciton transport to the polymer−semiconductor interface is inefficient when the adsorbed polymers exist as large multichain aggregates, resulting in reduced absorbed photon to current efficiencies (APCE).[7,8] The inefficient transport is believed to arise due to exciton trapping by the interchain aggregate states.[9,10] Clear analogies exist with bulk heterojunction materials, where charge separation and transport are correlated with the aggregation state of the conjugated polymer.[11−13] In contrast to this situation, individual, unaggregated CPE chains that are strongly coupled to a semiconductor interface are expected to efficiently inject electrons.[13,14]

Poly(phenylene ethynylene) CPEs have been widely investigated in hybrid photoelectrochemical cells because of their synthetic versatility and tunable band gaps, coupled with a substantial driving force (>0.5 eV) for injection of photoexcited electrons into the conduction band of oxide semiconductors such as rutile and anatase TiO_2.[7,8] However, a number of investigations have shown that this class of CPEs is prone to undergo aggregation in solution. In a previous study, we used high-resolution atomic force microscopy (AFM) to image the adsorption of a CPE onto single-crystal TiO_2 and found that the adsorbed polymer exists as aggregates that are believed to deposit from solution.[15−17] In recent work, we have uncovered an unusual structure−property relationship that guides the development of poly(phenylene ethynylene) CPEs that do not aggregate to a significant extent in solution.[18] Here, we use a CPE that is specifically designed so that it does not aggregate significantly in solution and study the morphology of the unaggregated polymer chains at an atomically flat single-crystal ZnO(0001) surface. Correlated AFM and photoelectrochemical studies reveal that the surface is dominated by individual polymer chains and that these unaggregated CPEs undergo efficient charge injection into ZnO.

The polymer used in this study (**poly-1**, Scheme 1) features a π-conjugated backbone comprised of alternating (1,4-phenylene ethynylene) and (2,5-thienylene ethynylene) repeats. The polar carboxylic acid substituents are linked to the phenylene

Scheme 1

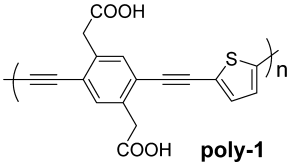

poly-1

Received: August 1, 2013
Accepted: September 10, 2013
Published: September 10, 2013

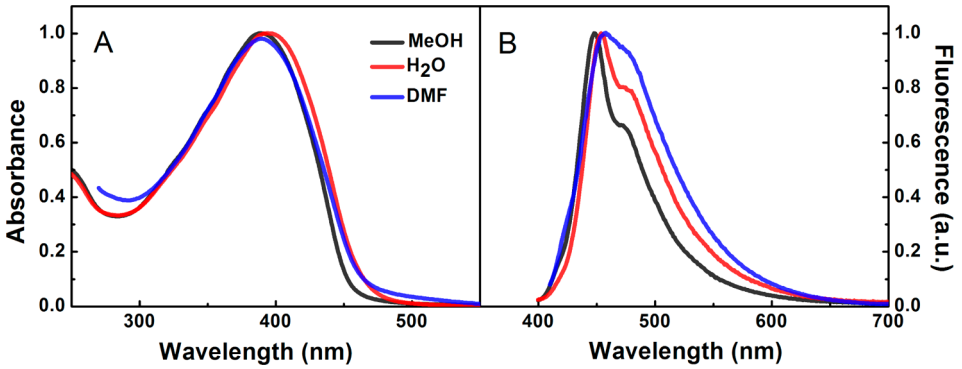

Figure 1. Absorption (A) and fluorescence (B) spectra for basic **poly-1** in MeOH (black), water (red), and **poly-1** in DMF (blue). MeOH contains 10 mM NaOH. H_2O at pH = 8.0.

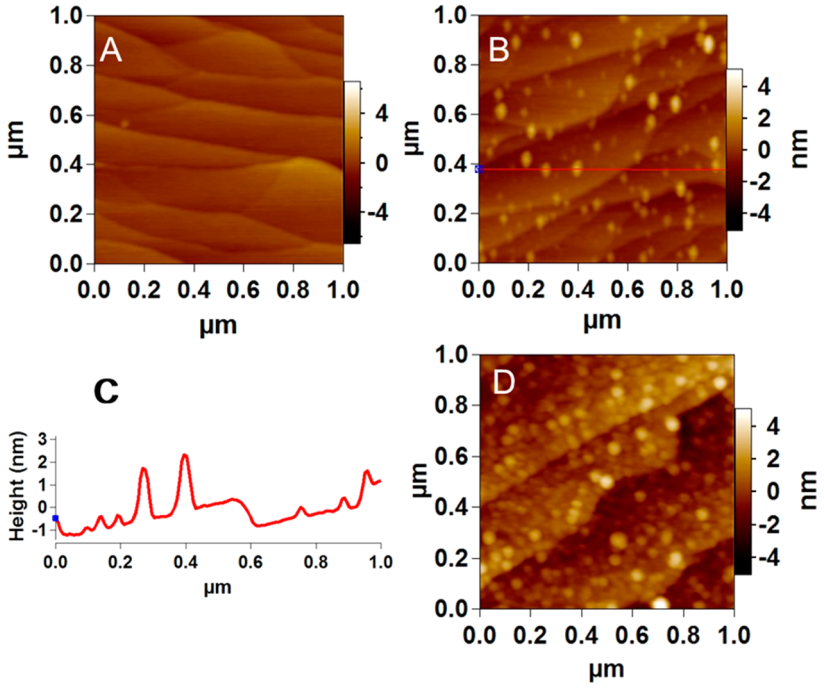

Figure 2. Noncontact tapping mode AFM images of **poly-1** deposited on a ZnO(0001) surface from DMF solutions of different concentrations with a dipping time of 5 min: (A) 0 (clean ZnO surface), (B) 6, and (D) 60 μg/mL. (C) Cross section analysis along the red line in (B).

rings via a single methylene unit ($-CH_2-$). In a separate study, we have shown that the use of the methylene linker, as opposed to oxy-methylene ($-O-CH_2-$), surprisingly reduces the tendency of the polymer to aggregate in solution.[18] The carboxylic acid substituted polymer was synthesized via a "precursor" route in which the carboxy units were protected as dodecyl esters. The ester precursor polymer is soluble in organic solvents, and GPC analysis indicates that it has a number average molecular weight (MW) of $M_n \approx 42$ kD, corresponding to a degree of polymerization of $X_n \approx 68$, with PDI ≈ 1.9 (full synthetic detail is provided in the Supporting Information). The acid form of the polymer was obtained by base-catalyzed hydrolysis of the esters, followed by acidification. Because the removal of the ester protecting groups does not affect the polymer backbone, the X_n value remains unchanged.

The photophysical properties of **poly-1** were characterized by UV−visible absorption and fluorescence spectroscopy in MeOH, H_2O, and DMF solutions (Figure 1). The polymer features a strongly allowed π,π^* absorption band with $\lambda_{max} \approx$ 388 nm and a structured fluorescence with $\lambda_{max} \approx$ 448 nm (values for MeOH solutions of the base form of **poly-1**) and a vibronic shoulder at longer wavelength. Interestingly, the absorption and fluorescence spectra of **poly-1** vary little with solvent, in contrast to the behavior of a structurally similar poly(1,4-phenylene ethynylene-*alt*-2,5-thienylene ethynylene) CPE, which features an $-O-CH_2-$ side-chain linker, where the absorption is red-shifted and the fluorescence is red-shifted and significantly reduced in intensity in water compared to that in methanol due to aggregation.[16] In contrast to the behavior of CPEs that aggregate in solution, **poly-1** exhibits very similar absorption and fluorescence spectra in MeOH, H_2O, and DMF with a comparatively large fluorescence quantum yield in all three solvents ($\phi_f \approx 0.26$, 0.17, and 0.30 in MeOH, H_2O, and DMF, respectively). These results strongly suggest that **poly-1** does not aggregate significantly in solution. The absence of significant aggregation is supported by Stern−Volmer fluorescence quenching studies that show relatively low K_{SV} values with methyl viologen and by fluorescence correlation spectroscopy (FCS), which affords diffusion times consistent with

dx.doi.org/10.1021/jz401636s | J. Phys. Chem. Lett. 2013, 4, 3216−3220

individually dissolved polymer chains (see the Supporting Information).

Carboxylic acid substituted CPEs can covalently bond to metal oxide interfaces, and their adsorption on mesoporous TiO_2 has been the focus of most investigations.[1,8] However, using AFM to obtain topographic information on the deposited CPE polymer chains within a mesoporous oxide film is challenging. Therefore, in this work, atomically flat n-type zinc oxide (0001) single-crystal surfaces were used as substrates (Figure 2A), allowing detailed structure determination with AFM and correlation of the photocurrent response with the adsorbed CPE morphology at the ZnO surface. In addition, ZnO is a semiconductor with a wide band gap of 3.2−3.4 eV,[19] which is suitable for studying sensitization by a wide range of organic dyes.[20] Given that the absorption λ_{max} for the polymer is 389 nm, corresponding to ∼3.1 eV, ZnO is more suitable for these studies due to its larger band gap compared to TiO_2 (E_g = 3.0−3.2 eV). In addition, we estimate that there is 0.2−0.4 eV of driving force for charge injection from the singlet excited state of **poly-1** into the ZnO conduction band.[21]

Figure 2A shows AFM images of a polished and annealed ZnO(0001) crystal surface, revealing the atomically flat terraces of height ∼100−300 pm and 250 nm width. The acid form of **poly-1** was adsorbed onto the ZnO electrode by immersion into DMF solution of various concentrations of the polymer for 5 min. This was found to be the most reliable and reproducible process for producing a uniform coverage of the polymer onto the single-crystal surfaces. Polymer adsorption from low concentrations of **poly-1** results in the appearance of submonolayer coverage of "particles" in the AFM images (Figure 2B) that we associate with the individual polymer chains. It is interesting that the morphology of the polymer structures at the ZnO interface appear as ellipsoidal particles, rather than rod-like structures (see Figure S4, Supporting Information). Cross section analysis along the horizontal red line across Figure 2B reveals that most of the particles are ∼2 nm in height (Figure 2C), consistent with the height expected for individual polymer chains (see below). Analysis of the particle heights in a typical AFM image reveals a mean and standard deviation of 1.8 ± 0.5 nm. Their size in the $x-y$ dimension is larger than expected for single polymer chains due to convolution of the particle dimension with the tip, which is considerably larger in size.[22,23] Exposure to a solution with higher polymer concentrations results in an increase of the surface coverage of ellipsoidal particles without apparent aggregation (Figure 2D). Close inspection of Figure 2D reveals that it is still possible to resolve most of the individual particles in the image, and in some cases, closely packed individual particles can be imaged on the ZnO surface.

To verify the premise that the features in the AFM images correspond to individual polymer chains, the distribution of particle sizes from the AFM images and the distribution of calculated radii for the polymer chains from GPC analysis were compared (Figure 3). The histogram showing the distribution of particle heights obtained by analysis of the AFM image in Figure 2B is shown in Figure 3A. The lower-coverage image was used because the particles are often touching at higher coverage and may not be as well-resolved in the AFM images. Particle heights were used to estimate their size because, as noted above, their diameter is influenced by convolution with the AFM tip radius. The distribution of AFM particle heights clusters around 2 nm with a distribution width of ±1 nm. The distribution of polymer chain radii values was calculated based

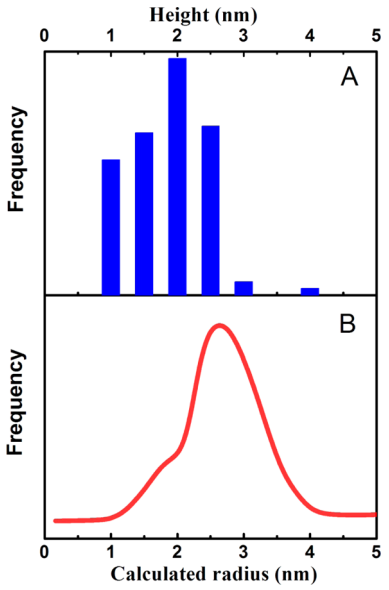

Figure 3. (A) Histogram showing the distribution of the feature heights obtained by analysis of the AFM image shown in Figure 2B. (B) Histogram showing the distribution of the calculated polymer chain radius from GPC analysis (see the Supporting Information for calculations).

on the polymer MW distribution derived from the analytical GPC curve by applying a hemispherical model (see equations in the Supporting Information), where the radius computed from the MW corresponds to the height (Figure 3B). The distribution of calculated polymer radii exhibits a similar trend compared to the AFM particle heights, with the average GPC calculated radius being ∼1 nm larger. The difference can be attributed to the fact that the polymer chains likely flatten upon adsorption onto the ZnO surface. Nevertheless, the qualitative correlation between the distribution of AFM particle heights and the calculated values of chain radii supports the premise that **poly-1** adsorbs to the ZnO surface as individual chains as opposed to larger aggregates consisting of multiple chains.

The above correlation of AFM images and GPC makes it apparent that the **poly-1** does not adsorb on the surface as a rigid-rod structure, but rather, it exists in a coiled conformation. Molecular dynamics (MD) simulations were carried out in order to provide more insight regarding the conformations accessible to **poly-1** in solution. Ten MD simulations were run for chains that contain 20 and 40 repeat units (1 μs trajectory for each run). In every case, the formation of a loop starting from one end of the chain was observed (see .mpg files in the Supporting Information). The initial contact was usually seen between the first repeat unit and the 13th repeat unit, after which winding into a helix proceeded very quickly. For a 40-mer, the diameter of the helix, as shown in Figure S6 (Supporting Information), was 4.7 ± 0.3 nm, while the height was 1.34 ± 0.2 nm. Projecting to the expected dimensions of 68 repeat units, according to the experimental polymer length, a height of 2.5 nm is predicted, which is in good agreement with the experimental AFM height data. Similar helical chain conformations were recently reported for simulations of the solution structure of poly-3-hexylthiophene using a coarse grain model,[24] where the driving force for self-aggregation is aromatic−aromatic interactions that in these cases are stronger than polymer−solvent energy terms and are needed to counter entropic effects.

dx.doi.org/10.1021/jz401636s | J. Phys. Chem. Lett. 2013, 4, 3216−3220

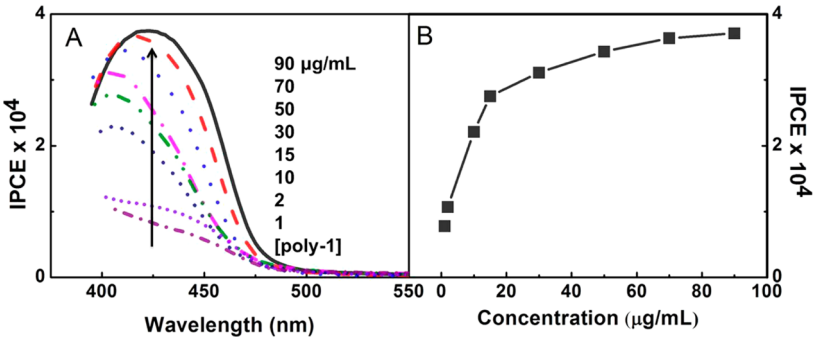

Figure 4. (A) IPCE spectra for a ZnO electrode dipped into various concentrations of **poly-1** in DMF solution for 5 min, corresponding to the times used in the AFM measurements. The peak photocurrent increases with **poly-1** concentration in the deposition solution (the legend shows the **poly-1** concentration in μg/mL). (B) IPCE values at 420 nm as a function of the dipping solution concentration. These experiments were carried out with the single-crystal electrode immersed in an aqueous solution of 20 mM KI, 0.1 M KNO_3, and pH 6, using a three-electrode setup with the potential of the working electrode held at 0 V versus a Ag/AgCl as a reference electrode.

In summary, there is reasonable agreement between the estimated size of individual **poly-1** chains based on analysis of GPC data and MD simulations and the experimental height of the particles imaged at the ZnO surface by AFM. Even though the size agreement is not quantitative, the results provide a compelling case that **poly-1** exists at the ZnO interface as single polymer chains wrapped in a coiled conformation.

Photocurrent spectroscopy was used to determine whether the lack of aggregation was also evident in the photoelectrochemical behavior of the polymer sensitizer. Figure 4A shows the incident photon to current efficiency (IPCE) spectra for adsorbed **poly-1** on the surfaces of ZnO(0001) single crystals from various **poly-1** concentrations with the same deposition times as those used to obtain the AFM images. The IPCE data were obtained with a three-electrode setup with the ZnO electrode immersed in aqueous electrolyte solution using Ag/AgCl as a reference electrode and a platinum wire as a counter electrode. Photocurrent can be measured at even the lowest **poly-1** coverage, indicating that photoinduced electron injection from the CPE to ZnO occurs even at the lowest coverage. The sensitized photocurrent from **poly-1** absorbed from DMF onsets at 480 nm and reaches a maximum value at ~410 nm.[25] The photocurrent increases with the **poly-1** concentration in the deposition solution, exhibiting a shape reminiscent of a Langmuir adsorption isotherm with a saturation point at ~30 μg/mL, as shown in Figure 4B. This isotherm-like behavior in photocurrent is similar to that observed for adsorption of monomeric ruthenium dyes and monomeric and H-aggregated cyanine dyes onto TiO_2 single-crystal surfaces (anatase and rutile).[26] The maximum IPCE for **poly-1** on the ZnO surfaces is ~0.04% (peak APCE ≈ 5% based on estimated absorption for a 2 nm thick monolayer film of **poly-1**). There are several explanations for the low IPCE values. First, even at saturation, the surface coverage corresponds to a monolayer of the polymer, and consequently, the film absorptance is low (<0.01). Second, the onset of the absorption by the ZnO crystal is at ~410 nm and overlaps with the absorption maximum of the polymer, attenuating the light absorbed by the sensitizer. It is important to note that the plateauing of the photocurrent at high polymer surface coverage and the absence of multilayers in the AFM images suggest that the individual **poly-1** chains are strongly electronically coupled to the ZnO surface and are not present as multilayer/aggregate structures at the interface. In contrast, for other CPE sensitizers, a decrease in the IPCE values is observed with increasing coverage due to the formation of multilayers where photoexcited carriers or excitons created near the polymer surface cannot reach the interface to be separated by electron injection into the semiconductor conduction band.[8]

In conclusion, we have studied the adsorption of a nonaggregating CPE onto single-crystal ZnO using AFM and photoelectrochemistry. The AFM images obtained at various surface coverages strongly support the premise that the polymer adsorbs from solution as single chains that are in a coiled conformation. Correlation of the feature sizes from AFM with the polymer radius computed from the GPC MW distribution are in relatively good agreement, supporting the single-chain adsorption model. MD simulations suggest that the coiled conformation could consist of a helical structure, stabilized by π-interactions and hydrogen bonding between the carboxylic acid groups. The adsorbed CPEs display a modest photocurrent, and due to the relatively low absorptance of the film, the results suggest that photoinduced charge injection by the adsorbed CPE chains is modestly efficient. Nonaggregating CPE sensitizers may be useful in designing more efficient solar cells as they allow for more control of surface morphology and electronic interaction between the semiconductor and polymer.

■ ASSOCIATED CONTENT

Ⓢ Supporting Information

Experimental procedures for monomer and polymer synthesis, molecular dynamics simulations, ZnO crystal preparation, AFM imaging, and photoelectrochemical measurements. Additional information and results includes plots of fluorescence correlation spectroscopy results, Stern−Volmer quenching results, GPC analysis and equations used to calculate polymer chain radius values, and polymer structure images and molecular dynamics trajectory (.mpg files). This material is available free of charge via the Internet at http://pubs.acs.org.

■ AUTHOR INFORMATION

Corresponding Authors

*E-mail: bparkin1@uwyo.edu (B.A.P.).
*E-mail: kschanze@chem.ufl.edu (K.S.S.).

Funding

This work was funded by the Division of Chemical Sciences, Geosciences, and Biosciences, Office of Basic Energy Sciences of the U.S. Department of Energy through Grant No. DE-FG03-96ER14625. Work at the University of Florida is

supported by the U.S. Department of Energy (Grant No. DE-FG02-03ER15484).

Notes

The authors declare no competing financial interest.

■ ACKNOWLEDGMENTS

We acknowledge Dr. Fude Feng and Dr. Jie Yang for assistance with the CPE synthesis and fluorescence correlation spectroscopy measurements.

■ REFERENCES

(1) Fang, Z.; Eshbaugh, A. A.; Schanze, K. S. Low-Bandgap Donor–Acceptor Conjugated Polymer Sensitizers for Dye-Sensitized Solar Cells. *J. Am. Chem. Soc.* **2011**, *133*, 3063–3069.

(2) Mwaura, J. K.; Zhao, X. Y.; Jiang, H.; Schanze, K. S.; Reynolds, J. R. Spectral Broadening in Nanocrytalline TiO_2 Solar Cells Based on Poly(*p*-Phenylene Ethynylene) and Polythiophene Sensitizers. *Chem. Mater.* **2006**, *18*, 6109–6111.

(3) Schanze, K. S.; Shelton, A. H. Functional Polyelectrolytes. *Langmuir* **2009**, *25*, 13698–13702.

(4) Jiang, H.; Taranekar, P.; Reynolds, J. R.; Schanze, K. S. Conjugated Polyelectrolytes: Synthesis, Photophysics, and Applications. *Angew. Chem., Int. Ed.* **2009**, *48*, 4300–4316.

(5) Takeda, N.; Parkinson, B. A. Adsorption Morphology, Light Absorption, and Sensitization Yields for Squaraine Dyes on SnS_2 Surfaces. *J. Am. Chem. Soc.* **2003**, *125*, 5559–5571.

(6) Ushiroda, S.; Ruzycki, N.; Lu, Y.; Spitler, M. T.; Parkinson, B. A. Dye Sensitization of the Anatase (101) Crystal Surface by a Series of Dicarboxylated Thiacyanine Dyes. *J. Am. Chem. Soc.* **2005**, *127*, 5158–5168.

(7) Jiang, H.; Zhao, X. Y.; Shelton, A. H.; Lee, S. H.; Reynolds, J. R.; Schanze, K. S. Variable-Band-Gap Poly(arylene ethynylene) Conjugated Polyelectrolytes Adsorbed on Nanocrystalline TiO_2: Photocurrent Efficiency as a Function of the Band Gap. *ACS Appl. Mater. Interfaces* **2009**, *1*, 381–387.

(8) Sambur, J. B.; Averill, C. M.; Bradley, C.; Schuttlefield, J.; Lee, S. H.; Reynolds, J. R.; Schanze, K. S.; Parkinson, B. A. Interfacial Morphology and Photoelectrochemistry of Conjugated Polyelectrolytes Adsorbed on Single Crystal TiO_2. *Langmuir* **2011**, *27*, 11906–11916.

(9) Wenger, B.; Gratzel, M.; Moser, J. E. Rationale for Kinetic Heterogeneity of Ultrafast Light-Induced Electron Transfer from Ru(II) Complex Sensitizers to Nanocrystalline TiO_2. *J. Am. Chem. Soc.* **2005**, *127*, 12150–12151.

(10) Hamann, T. W.; Jensen, R. A.; Martinson, A. B. F.; Van Ryswyk, H.; Hupp, J. T. Advancing Beyond Current Generation Dye-Sensitized Solar Cells. *Energ. Environ. Sci.* **2008**, *1*, 66–78.

(11) Yang, X.; Loos, J. Toward High-Performance Polymer Solar Cells: The Importance of Morphology Control. *Macromolecules* **2007**, *40*, 1353–1362.

(12) Schubert, M.; Dolfen, D.; Frisch, J.; Roland, S.; Steyrleuthner, R.; Stiller, B.; Chen, Z.; Scherf, U.; Koch, N.; Facchetti, A.; Neher, D. Influence of Aggregation on the Performance of All-Polymer Solar Cells Containing Low-Bandgap Naphthalenediimide Copolymers. *Adv. Energy Mater* **2012**, *2*, 369–380.

(13) Groves, C.; Reid, O. G.; Ginger, D. S. Heterogeneity in Polymer Solar Cells: Local Morphology and Performance in Organic Photovoltaics Studied with Scanning Probe Microscopy. *Acc. Chem. Res.* **2010**, *43*, 612–620.

(14) Giridharagopal, R.; Shao, G. Z.; Groves, C.; Ginger, D. S. New SPM Techniques for Analyzing OPV Materials. *Mater. Today* **2010**, *13*, 50–56.

(15) Tan, C. Y.; Pinto, M. R.; Schanze, K. S. Photophysics, Aggregation and Amplified Quenching of a Water-Soluble Poly(phenylene ethynylene). *Chem. Commun.* **2002**, 446–447.

(16) Zhao, X. Y.; Pinto, M. R.; Hardison, L. M.; Mwaura, J.; Muller, J.; Jiang, H.; Witker, D.; Kleiman, V. D.; Reynolds, J. R.; Schanze, K. S. Variable Band Gap Poly(arylene ethynylene) Conjugated Polyelectrolytes. *Macromolecules* **2006**, *39*, 6355–6366.

(17) Zhao, X. Y.; Liu, Y.; Schanze, K. S. A Conjugated Polyelectrolyte-Based Fluorescence Sensor for Pyrophosphate. *Chem. Commun.* **2007**, 2914–2916.

(18) Xie, D. P.; Parthasarathy, A.; Schanze, K. S. Aggregation-Induced Amplified Quenching in Conjugated Polyelectrolytes with Interrupted Conjugation. *Langmuir* **2011**, *27*, 11732–11736.

(19) Tiwana, P.; Docampo, P.; Johnston, M. B.; Snaith, H. J.; Herz, L. M. Electron Mobility and Injection Dynamics in Mesoporous ZnO, SnO_2, and TiO_2 Films Used in Dye-Sensitized Solar Cells. *ACS Nano* **2011**, *5*, 5158–5166.

(20) Anta, J. A.; Guillen, E.; Tena-Zaera, R. ZnO-Based Dye-Sensitized Solar Cells. *J. Phys. Chem. C* **2012**, *116*, 11413–11425.

(21) The driving force is estimated based on the reduction potential of **poly-1** (≈−1.1 V versus SCE, ref 8), the conduction band position of ZnO (≈−0.5 V versus SCE), and the exciton binding energy (≈0.3 eV).

(22) Raposo, M.; Ferreira, Q.; Riberio, P. A. In *Modern Research and Educational Topics in Microscopy*; Mendez-Vilas, A., Diaz, J., Eds.; FORMATEX: Badajoz, Spain, 2007; pp 758–769.

(23) Nepomnyashchii, A. B.; Parkinson, B. A. Influence of the Aggregation of a Carbazole Thiophene Cyanoacrylate Sensitizer on Sensitized Photocurrents on ZnO Single Crystals. *Langmuir* **2013**, *29*, 9362–9368.

(24) Schwarz, K. N.; Kee, T. W.; Huang, D. M. Coarse-Grained Simulations of the Solution-Phase Self-Assembly of Poly(3-hexylthiophene) Nanostructures. *Nanoscale* **2013**, *5*, 2017–2027.

(25) The peak IPCE response occurs at a longer wavelength compared to the absorption maximum of the polymer. This is likely due to an artifact caused by attenuation of the incident light for wavelengths < 400 nm due to the onset of the ZnO absorption.

(26) Lu, Y. F.; Choi, D. J.; Nelson, J.; Yang, O. B.; Parkinson, B. A. Adsorption, Desorption, and Sensitization of Low-Index Anatase and Rutile Surfaces by the Ruthenium Complex Dye N3. *J. Electrochem. Soc.* **2006**, *153*, E131–E137.